

Reconstruction of asteroid spin states from Gaia DR2 photometry

J. Ďurech¹ and J. Hanuš¹

Astronomical Institute, Faculty of Mathematics and Physics, Charles University, V Holešovičkách 2, 180 00 Prague 8, Czech Republic
e-mail: durech@sirrah.troja.mff.cuni.cz

Received ?; accepted ?

ABSTRACT

Context. In addition to stellar data, Gaia Data Release 2 (DR2) also contains accurate astrometry and photometry of about 14,000 asteroids covering 22 months of observations.

Aims. We used Gaia asteroid photometry to reconstruct rotation periods, spin axis directions, and the coarse shapes of a subset of asteroids with enough observations. One of our aims was to test the reliability of the models with respect to the number of data points and to check the consistency of these models with independent data. Another aim was to produce new asteroid models to enlarge the sample of asteroids with known spin and shape.

Methods. We used the lightcurve inversion method to scan the period and pole parameter space to create final shape models that best reproduce the observed data. To search for the sidereal rotation period, we also used a simpler model of a geometrically scattering triaxial ellipsoid.

Results. By processing about 5400 asteroids with at least ten observations in DR2, we derived models for 173 asteroids, 129 of which are new. Models of the remaining asteroids were already known from the inversion of independent data, and we used them for verification and error estimation. We also compared the formally best rotation periods based on Gaia data with those derived from dense lightcurves.

Conclusions. We show that a correct rotation period can be determined even when the number of observations N is less than 20, but the rate of false solutions is high. For $N > 30$, the solution of the inverse problem is often successful and the parameters are likely to be correct in most cases. These results are very promising because the final Gaia catalogue should contain photometry for hundreds of thousands of asteroids, typically with several tens of data points per object, which should be sufficient for reliable spin reconstruction.

Key words. Minor planets, asteroids: general, Methods: data analysis, Techniques: photometric

1. Introduction

The ESA Gaia mission (Gaia Collaboration et al. 2016b) has been in the science operations phase since August 2014. So far, there have been two Data Releases, the first in September 2016 (DR1, Gaia Collaboration et al. 2016a) and the second in April 2018 (DR2, Gaia Collaboration et al. 2018a). The main output of DR2 is accurate astrometric data for more than a billion stars. However, unlike DR1, DR2 also contains astrometric and photometric data for about 14,000 asteroids (Gaia Collaboration et al. 2018b).

Time-resolved photometry of asteroids, i.e. lightcurves, can be used for the reconstruction of the rotation period, spin axis orientation, and shape (Kaasalainen et al. 2002; Ďurech et al. 2007a; Hanuš et al. 2016; Marciniak et al. 2007, 2018; Michałowski et al. 2004; Kryszczyńska 2013, for example). Also, photometry that is sparse in time with respect to the rotation period can be successfully used with the same lightcurve inversion method (Kaasalainen 2004; Ďurech et al. 2007b, 2009, 2016; Hanuš et al. 2011, 2013). Gaia provides this type of sparse-in-time photometry with unprecedented accuracy. After the end of mission, these data will be used to determine periods, spins, and triaxial shape models (Cellino et al. 2006, 2007; Cellino & Dell’Oro 2012; Santana-Ros et al. 2015). As shown by Santana-Ros et al. (2015), the probability of deriving a correct spin model is related to the shape (spherical asteroids have small lightcurve amplitudes), spin axis latitude (low-latitude asteroids are sometimes seen pole-on with small lightcurve amplitude), and the

number of data points. Until now, real Gaia asteroid photometry was not available and the performance of inversion techniques was tested on simulated data. DR2 has changed this situation and we can now use real high-quality Gaia photometry and test whether the expectations were met. Here we use asteroid photometry released in DR2 with the aim of testing the limits of lightcurve inversion and the information content of the data. We also derive new asteroid models.

2. Inversion of Gaia asteroid photometry

The DR2 contains G-band brightness measurements with uncertainties for about 14,000 asteroids. The observations cover 22 months and the number of data points per object varies from a few to 50. As described by Gaia Collaboration et al. (2018b), the reported brightness values are constant for a single transit and they were computed as average values over the transit. Gaia Collaboration et al. (2018b) also tested the accuracy of the asteroid photometry and reached the conclusion that it is probably better than 1–2%. This is much better than the accuracy of sparse photometry from ground-based surveys, which is hardly better than 0.1 mag (Ďurech et al. 2009). A unique reconstruction of the shape/spin model is possible only if there are enough photometric data points with good accuracy covering a sufficiently wide interval of geometries. With ground-based surveys, the poor photometric quality is compensated with the number of data points, typically several hundred, observed over many apparitions. Even so, unique solutions are rare; the success rate of deriving a robust

and reliable model is less than one percent (Ďurech et al. 2016). In the case of Gaia, the final catalogue will contain data that fulfil all three requirements: they will be very accurate, there will be several tens of measurements per object, and they will cover several apparitions for a typical main-belt asteroid. According to simulations, several tens of accurate measurements should be sufficient to derive a unique spin solution and an approximate shape (Santana-Ros et al. 2015).

DR2 photometry allowed us to test how successful the inversion of real Gaia data is. We selected all 5413 asteroids for which the number of brightness measurements N was ≥ 10 . We computed the geometry with respect to the Sun and the Gaia spacecraft for each observation and processed the data in the same way as in Hanuš et al. (2011) and Ďurech et al. (2016, 2018) by using the lightcurve inversion method of Kaasalainen et al. (2001). Our approach is similar to that of Torppa et al. (2018) with the main difference that we do not deal with any error analysis. For each processed asteroid, we searched for a shape/spin model that gives the best fit to the data, measured by the lowest χ^2 between the observed and modelled brightness. All data points were given the same weight; we did not take into account errors of individual measurements. The reason was that the relative formal errors are mostly below 2% (90% of all data points), and in this range the difference between, for example, 1% and 0.1% accuracy plays no role because the errors introduced by the model are larger (simplified shape approximation and scattering model assuming uniform albedo).

2.1. Rotation periods

As the first step, we computed periodograms using convex shapes and ellipsoids and tested the reliability of the formally best-fit period. In Fig. 1, we show the comparison between the best period derived from DR2 using either convex shapes or ellipsoids and the values compiled in the Lightcurve Database (LCDB) of Warner et al. (2009); we used the version from November 12, 2017. We used only reliable LCDB periods with the uncertainty code $U \geq 3$. The colour-coding correlates with the number of data points N . Convex models do not provide any periods when $N \leq 20$ (see the discussion below). The points concentrating on the diagonal line represent the correctly determined periods (Gaia and LCDB periods are the same). The points off the diagonal are likely incorrect Gaia periods because LCDB records with $U \geq 3$ should be reliable. The minor diagonal in the left panel are false solutions with the derived period being half of the real one; this can happen with convex shapes as they produce lightcurves with only one minimum/maximum per rotation. Ellipsoidal models do not have this disadvantage of producing false half periods, but the periods based on a small number of points are often wrong. In general, when there are more data points, it is more likely that the derived period will be correct.

The dependence of the number of false periods on the number of data points is shown in Fig. 2. The fraction of correctly determined periods (defined as those that agree with LCDB values within $\pm 5\%$) increases above 0.5 when $N > 30$. For fewer points, the formally best periods are not reliable. The clustering of points around shorter periods is likely a consequence of the way the model is constructed; it is easier to formally fit the sparse points with an incorrect period that is shorter than the true period. For $N > 40$, the success rate seems to be high, but the sample size of asteroids in this range is very small.

We also tested if there is any difference in the photometric errors of Gaia data between the asteroids with correctly and incorrectly determined rotation periods. For the two bins with N between 21–25 and 26–30 (where the fraction of correctly determined periods is about 50% and the number of periods is large), we compared the photometric errors of points belonging to asteroids with correctly determined periods with those that belong to asteroids with incorrect Gaia-based periods. The t-test did not reveal any significant difference in the means of these two groups. Also, the distribution of observations in time was very similar for the two groups. We did not reveal any statistical difference in, for example, the number of observations separated by ~ 100 minutes, which is the spacing related to the scanning pattern of Gaia corresponding to two field-of-view transits.

2.2. Spins and shapes

The best-fit periods discussed above are often just random global minima in the periodograms. To distinguish between random and real periods, we have to define some level of significance measured by the χ^2 fit. We defined the uniqueness of the best solution by the depth of the χ^2 minimum with respect to other local minima. The formula we used for the threshold $\chi_{\text{tr}}^2 = (1 + \sqrt{2/\nu})\chi_{\text{min}}^2$ is a modification of the formula we used in Ďurech et al. (2018); now there is no factor of 1/2. This is an arbitrary borderline that is based on a trade-off between the total number of new models and their contamination with incorrect models. Here ν is the number of degrees of freedom, which is formally the difference between the number of points N and the number of parameters p . For ellipsoids, $p = 6$ and the parameters are the sidereal rotation period P , the spin axis direction in ecliptic coordinates λ and β , one parameter for the linear slope of the phase curve, and two parameters (a/c and b/c) for the ellipsoid axes ratios. With Gaia observations the phase angle is almost always > 10 deg, which means that the phase function can be reduced to only a linear part with one parameter (Kaasalainen et al. 2001). With convex models, we used the spherical harmonics representation of the order and degree of three (Kaasalainen et al. 2001), which corresponds to 16 shape parameters, so the total number of parameters is $p = 20$. For spin/shape reconstruction, we only used asteroids with $N > 20$.

When the number of points was small, in many cases we obtained RMS residuals of almost zero for many different periods. Such periodograms were excluded from the analysis. To avoid fitting noise, we only selected periodograms with all RMS values > 0.005 mag. Another requirement was that there should be only one period with RMS below 0.01. If there were more, we considered it a non-unique solution even if the threshold limit was satisfied. The verification procedure was the same as in Ďurech et al. (2018), see Fig. 3 there, with the only difference that we did not use $n = 6$ for the degree and order of the spherical harmonics series. The visual inspection of the periodograms was crucial because in many cases we obtained false solutions for $P \lesssim 3$ h or $P \gtrsim 100$ h. Even with a correct rotation period and pole, the corresponding shapes were often unrealistic with sharp edges and triangular pole-on silhouettes. This is a consequence of the order and degree of the spherical harmonics series ($n = 3$) being too low, but with a small number of photometric points there is not enough information to reconstruct higher resolution models. In this sense, convex shape models derived from DR2 data should not be taken as real shapes; they are just models that fit the data best with the given resolution, and they are likely to change significantly when more data points are available and a

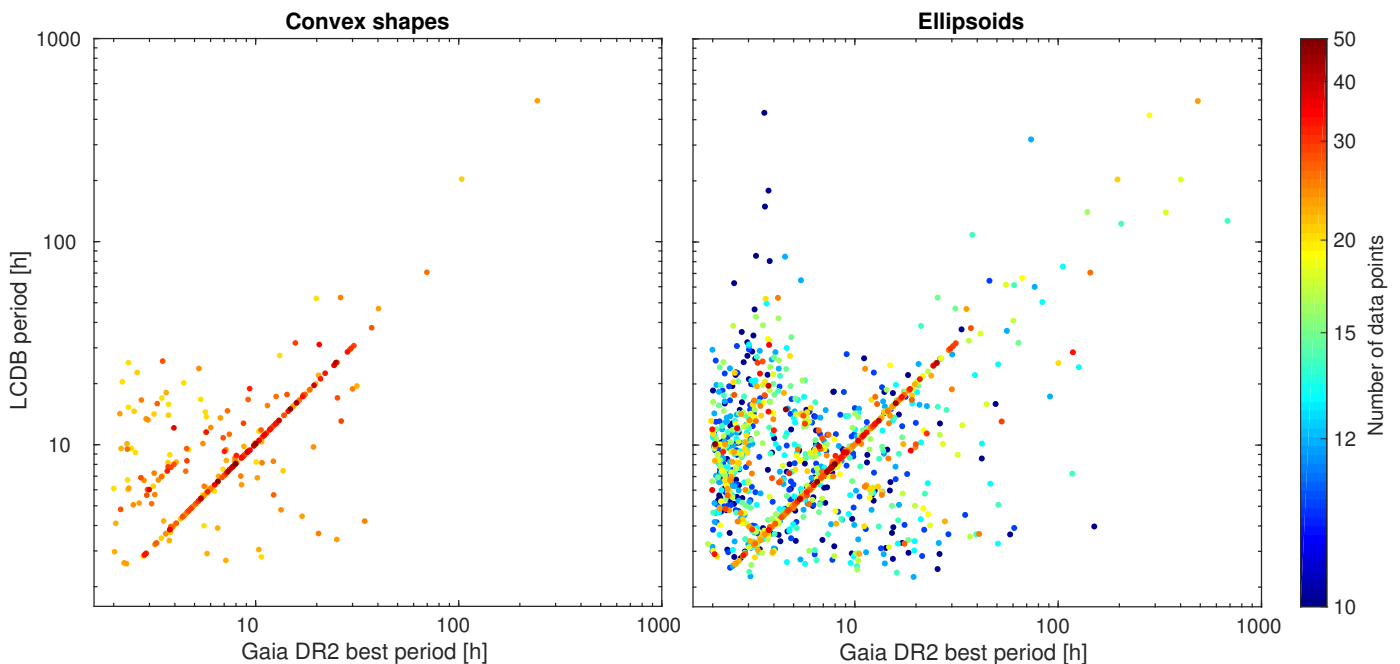


Fig. 1. Comparison between the best period derived from Gaia photometry with convex models (left) and ellipsoids (right). Each point represents an asteroid for which the best-fitting period from Gaia was determined and with a period in the LCDB with the uncertainty code $U \geq 3$. The number of Gaia observations N is expressed by the colour. The left panel contains fewer points because convex models were used only when $N > 20$.

higher degree of resolution is possible. On the other hand, the rotation periods and pole directions are not that sensitive to the resolution and they are more reliable (Hanus̆ & Ďurech 2012).

2.3. Comparison with independent models

By processing all asteroids with $N > 20$ and rejecting unreliable solutions, we derived models of 173 asteroids. Of these, 44 were already in the Database of Asteroid Models from Inversion Techniques (DAMIT, Ďurech et al. 2010) and we used them for an independent test of the accuracy of our solutions based on DR2. Most of our models agreed with those in DAMIT: their periods were the same within the errorbars and the mean difference between their pole directions was 20° . However, there was a group of clear outliers with differences between pole directions $> 60^\circ$. We looked in detail into these cases (seven in total). In one case – asteroid (2802) Weisell – the DAMIT model based only on sparse data (Hanus̆ et al. 2016) was clearly incorrect because the period search was done in the wrong local minimum. We removed this model from DAMIT. In five cases, the periods were very similar but differed more than their uncertainty, so the DR2-based solution was apparently a different local minimum leading to a different pole. In one case, the periods were completely different.

2.4. New models

In Table A.1, we list 129 new models and their spin axis directions (sometimes there are two possible solutions), the sidereal rotation period, and the period reported in the LCDB. The LCDB period agrees with our value in most cases. The asteroids for which the periods do not agree and the LCDB period is reliable (higher uncertainty code U) are marked with an asterisk.

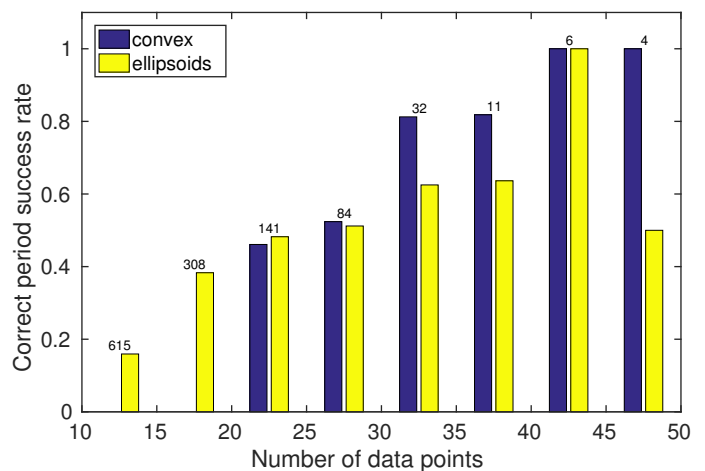


Fig. 2. Success rate of deriving correct rotation periods (compared with LCDB) for ellipsoidal and convex models. The number above each histogram bar is the number of asteroids with periods in the LCDB with $U \geq 3$ in that interval of data points.

To further check the reliability of these new models, we repeated the period search using reduced data sets. For each asteroid from Table A.1, we randomly selected and removed 10% of the data points (i.e. 2–5 points) from the original data set. In most cases, this reduction had no effect and the new periodogram showed the same unique period. In 44 cases, the reduced data set still provided the same best period, but it did not pass the threshold limit and thus was not considered a unique solution. In one case the new period was different from the original one. These asteroids are marked with an exclamation mark. This test shows that with our definition of χ_{tr}^2 , we are at the critical limit of the number of data points in many cases. Removing just a few points

may lead to formal rejection of the model even if it is correct (as is independently confirmed by the agreement between P and P_{LCDB}).

Because the geometry of observations is restricted mostly to the ecliptic plane, the lightcurve inversion usually produces two mirror shape solutions with about the same pole latitude β and the difference in longitude of $\sim 180^\circ$ (Kaasalainen & Lamberg 2006). However, there are a surprising number of solutions with just one pole direction in Table A.1 (compared with the results of Āurech et al. 2018, for example). This is likely caused by loosely constrained shapes that often are too elongated along the rotation axis. These shapes are removed by the pipeline. It means that the mirror pole solutions cannot be rejected even if they are not listed in Table A.1.

3. Discussion

Our analysis of Gaia DR2 asteroid photometry shows that the excellent photometric accuracy enables us to derive reliable spin directions and rotation periods from the first 22 months of Gaia observations. Although the number of unique models derived from DR2 is small compared to the number of all asteroids with photometry, this is mainly because the number of asteroids with ≥ 30 measurements is still limited. However, the prospect for the next data releases is very high. With more than 50 points covering several years, the inversion should provide unique results in most cases (apart from very spherical asteroids or those with extreme rotation) and the shape models will be more robust. Moreover, the photometric calibration in the future data releases should be even more accurate due to further improvement of the reduction pipeline that in the case of DR2 did not include correction for flux loss due to moving objects or a more sophisticated filtering of outliers, for example (Gaia Collaboration et al. 2018b).

Before DR3 (likely in the first half of 2021), the full potential of DR2 can be exploited when Gaia photometry is combined with archived lightcurves or sparse photometry from ground-based surveys. In this way, even a small number of accurate Gaia photometric measurements with a higher statistical weight can help to reconstruct uniquely the shape and spin state of many asteroids with the lightcurve inversion method.

Acknowledgements. The authors were supported by the grant no. 18-04514J of the Czech Science Foundation. This work has made use of data from the European Space Agency (ESA) mission *Gaia* (<https://www.cosmos.esa.int/gaia>), processed by the *Gaia* Data Processing and Analysis Consortium (DPAC, <https://www.cosmos.esa.int/web/gaia/dpac/consortium>). Funding for the DPAC has been provided by national institutions, in particular the institutions participating in the *Gaia* Multilateral Agreement.

References

- Cellino, A., Delbò, M., Zappalà, V., Dell’Oro, A., & Tanga, P. 2006, *Advances in Space Research*, 38, 2000
- Cellino, A. & Dell’Oro, A. 2012, *Planet. Space Sci.*, 73, 52
- Cellino, A., Tanga, P., Dell’Oro, A., & Hestroffer, D. 2007, *Advances in Space Research*, 40, 202
- Āurech, J., Hanuš, J., & Alf-Lagoa, V. 2018, *A&A*, 617, A57
- Āurech, J., Hanuš, J., Oszkiewicz, D., & Vančo, R. 2016, *A&A*, 587, A48
- Āurech, J., Kaasalainen, M., Marciniak, A., et al. 2007a, *A&A*, 465, 331
- Āurech, J., Kaasalainen, M., Warner, B. D., et al. 2009, *A&A*, 493, 291
- Āurech, J., Scheirich, P., Kaasalainen, M., et al. 2007b, in *Near Earth Objects, our Celestial Neighbors: Opportunity and Risk*, ed. A. Milani, G. B. Valsecchi, & D. Vokrouhlický (Cambridge: Cambridge University Press), 191
- Āurech, J., Sidorin, V., & Kaasalainen, M. 2010, *A&A*, 513, A46
- Gaia Collaboration, Brown, A. G. A., Vallenari, A., et al. 2018a, *A&A*, 616, A1
- Gaia Collaboration, Brown, A. G. A., Vallenari, A., et al. 2016a, *A&A*, 595, A2

- Gaia Collaboration, Prusti, T., de Bruijne, J. H. J., et al. 2016b, *A&A*, 595, A1
- Gaia Collaboration, Spoto, F., Tanga, P., et al. 2018b, *A&A*, 616, A13
- Hanuš, J. & Āurech, J. 2012, *Planet. Space Sci.*, 73, 75
- Hanuš, J., Āurech, J., Brož, M., et al. 2013, *A&A*, 551, A67
- Hanuš, J., Āurech, J., Brož, M., et al. 2011, *A&A*, 530, A134
- Hanuš, J., Āurech, J., Oszkiewicz, D. A., et al. 2016, *A&A*, 586, A108
- Kaasalainen, M. 2004, *A&A*, 422, L39
- Kaasalainen, M. & Lamberg, L. 2006, *Inverse Problems*, 22, 749
- Kaasalainen, M., Torppa, J., & Muinonen, K. 2001, *Icarus*, 153, 37
- Kaasalainen, M., Torppa, J., & Piironen, J. 2002, *Icarus*, 159, 369
- Kryszczyńska, A. 2013, *A&A*, 551, A102
- Marciniak, A., Bartczak, P., Müller, T., et al. 2018, *A&A*, 610, A7
- Marciniak, A., Michałowski, T., Kaasalainen, M., et al. 2007, *A&A*, 473, 633
- Michałowski, T., Kwiatkowski, T., Kaasalainen, M., et al. 2004, *A&A*, 416, 353
- Santana-Ros, T., Bartczak, P., Michałowski, T., Tanga, P., & Cellino, A. 2015, *MNRAS*, 450, 333
- Torppa, J., Granvik, M., Penttilä, A., et al. 2018, *Advances in Space Research*, 62, 464
- Warner, B. D., Harris, A. W., & Pravec, P. 2009, *Icarus*, 202, 134

Appendix A: List of new models

Table A.1. List of new asteroid models. For each asteroid, we list one or two pole directions in the ecliptic coordinates (λ, β), the sidereal rotation period P , the rotation period from LCDB P_{LCDB} (if available) and its quality code U , the number N of sparse photometric data points in DR2, and the method used to derive the rotation period: C – convex inversion, E – ellipsoids, CE – both methods gave the same unique period. The accuracy of the sidereal rotation period P is of the order of the last decimal place given. For asteroids marked with an asterisk, there is an inconsistency between P and P_{LCDB} and those marked with an exclamation mark did not pass the χ^2_{tr} limit when 10% of points were removed.

number	Asteroid name/designation	λ_1 [deg]	β_1 [deg]	λ_2 [deg]	β_2 [deg]	P [h]	P_{LCDB} [h]	U	N	method
205	Martha	358	-35			14.9117	14.911	3	46	C
! 217	Eudora	131	-4	317	11	25.262	25.272	3	29	C
333	Badenia	3	-48	179	-27	9.8609	9.862	3	25	CE
561	Ingwelde	89	68			12.0118	12.012	3	22	C
580	Selene	62	66	269	50	9.4929	9.47	3-	34	C
581	Tauntonia	203	-49			24.994	16.54	2	32	C
659	Nestor	6	-83			15.979	15.98	3	42	C
! 723	Hammonia	146	22	330	21	5.4348	5.436	3	31	CE
* ! 838	Seraphina	18	4	192	32	11.7245	15.67	2	28	C
! 842	Kerstin	18	78			18.716			23	CE
876	Scott	105	-18	262	-35	11.8178	11.814	2	27	E
906	Repsolda	108	-48			15.367	15.368	3	23	E
961	Gunnie	37	24	220	7	21.361			23	CE
976	Benjamina	354	80			9.7080	9.700	3-	23	E
1029	La Plata	119	30	274	44	15.3101	15.310	3	21	C
! 1107	Lictoria	82	57	303	57	8.5610	8.5616	3	31	CE
1118	Hanskya	224	-87			25.305	15.61	2	39	C
* ! 1165	Imprinetta	39	-82			10.8087	8.107	3	25	C
! 1168	Brandia	310	65			11.4425	11.444	3	21	E
! 1220	Crocus	26	48	165	80	488.6	491.4	3	23	E
1431	Luanda	79	54			4.13591	4.141	3-	23	E
1437	Diomedes	320	1			24.501	24.49	3-	26	E
1533	Saimaa	332	-70			7.1174	7.08	3	25	C
* ! 1540	Kevola	96	-71			5.00453	20.082	3-	32	E
1542	Schalen	92	41	268	52	7.5153	7.516	3	23	E
! 1604	Tombaugh	166	34	323	36	7.0359	7.047	2+	35	CE
! 1647	Menelaus	157	26	330	23	17.745	17.74	3-	28	E
! 1762	Russell	8	89			12.7933	12.797	3-	22	C
! 1767	Lampland	186	-53	340	-47	35.399			29	CE
* ! 1786	Raabe	88	45			30.175	18.72	3	25	C
! 1799	Koussevitzky	58	-61			6.3256	6.318	3	22	E
1849	Kresak	140	61			31.716	19.101	2	27	E
1873	Agenor	117	56			20.631	20.60	2	26	E
! 1939	Loretta	21	-72	201	-72	23.931	25.	1	33	CE
! 1975	Pikelnr	74	38			11.2768			32	C
2090	Mizuho	231	-22			5.4793	5.47	2+	22	E
2104	Toronto	306	-74			8.9667	8.97	3	24	E
2111	Tselina	102	19	282	53	6.5631	6.563	3	46	C
! 2127	Tanya	64	61			7.8523	7.864	2	35	CE
2147	Kharadze	180	-13	347	-45	14.1384	14.115	2	26	CE
2192	Pyatigoriya	139	44	338	81	8.7162			27	C
2203	van Rhijn	63	-76			30.607	30.55	2	21	E
2230	Yunnan	2	64	154	73	10.0381			21	E
! 2386	Nikonov	52	51	242	33	5.8944			21	E
2397	Lappajarvi	77	-55	251	-35	9.0532	9.05	2	28	C
2429	Schurer	235	-26			6.5119	6.66	3-	42	CE
! 2587	Gardner	351	49			11.6268	11.631	2	30	E
2627	Churyumov	141	-45	307	-70	7.6531	7.66	3-	29	CE
2634	James Bradley	120	-58			16.514			21	E
2683	Brian	112	-34	294	-50	22.528			33	CE
2686	Linda Susan	51	-52	268	-78	8.7222			31	C
* 2760	Kacha	101	-30			53.040	13.0	3	29	E
2884	Reddish	201	-84			35.537			26	CE
3131	Mason-Dixon	294	57			19.703	19.748	2	41	C
3134	Kostinsky	276	88			14.6755	14.7	2	41	CE
3210	Lupishko	42	55			14.2490	14.241	2	35	E
3325	TARDIS	142	-50	338	-79	11.5681			48	CE
3374	Namur	217	34			13.8542			27	C
! 3420	Standish	355	76			10.3869			25	CE
3451	Mentor	81	18			7.6966	7.702	3	29	E
! 3525	Paul	10	-3	214	27	13.4116	12.	2-	21	C
3565	Ojima	99	66	294	68	15.4510			32	C

Table A.1. continued.

number	Asteroid name/designation	λ_1 [deg]	β_1 [deg]	λ_2 [deg]	β_2 [deg]	P [h]	P_{LCDB} [h]	U	N	method
! 3776	Vartiouvuori	190	-83			11.3414	7.7	2-	24	E
3788	Steyaert	67	-86			29.966			29	CE
! 4075	Sviridov	17	89	329	62	6.6626			22	C
4131	Stasik	31	-64	203	-70	16.5405			25	CE
4271	Novosibirsk	105	58	320	60	8.8469	8.850	3	27	CE
! 4352	Kyoto	155	42	341	28	21.922	21.9352	3-	32	CE
! 4366	Venikagan	14	38	188	37	60.48			32	C
4369	Seifert	15	-30	170	-56	30.617	30.573	3	29	C
! 4451	Grieve	177	-68	341	-63	6.8600	6.864	3	28	E
! 4575	Broman	181	-66	303	-61	10.7735			26	CE
4613	Mamoru	280	-53			5.38872	5.388	3	41	CE
4732	Froeschle	105	-25	289	-24	12.0479			26	E
! 4930	Rephiltim	264	-72			5.24273	5.243	3	30	CE
! 5059	Saroma	33	-59	215	-30	4.0744	4.074	3	22	E
5130	Ilioneus	128	-19	303	-8	14.7357	14.768	3	22	E
5138	Gyoda	157	-90			8.4159			23	E
! 5285	Krethon	182	-89			12.0247	12.04	2	24	E
5344	Ryabov	9	90	286	71	18.490			26	E
! 5385	Kamenka	168	23			6.6719	6.683	2	25	E
5594	Jimmiller	260	-31			25.275	25.264	2	26	C
5755	1992 OP7	51	78	190	88	5.5752			29	E
5883	Josephblack	38	7	228	21	17.542			27	CE
6173	Jimwestphal	93	-30			2.90849	2.908	3	27	C
6338	Isaosato	146	84			4.97689			30	CE
6665	Kagawa	40	-36			6.7494			24	E
! 6794	Masuisakura	154	-29	345	-57	4.58811	4.58	3	23	E
! 7022	1992 JN4	4	84	337	56	5.5154	5.517	2	28	E
7238	Kobori	42	-83	238	-88	17.2242			37	C
7457	Veselov	16	88			12.2002			25	E
7458	1984 DE1	48	39	232	17	15.7543	16.7	2	25	C
! 7616	Sadako	185	-70	339	-37	11.0085			24	C
! 7650	Kaname	58	-86			18.177	18.172	2	24	CE
! 8066	Poldimeri	205	-69	342	-88	18.420			28	E
8292	1992 SU14	32	20			19.802	2.856	1	25	E
8443	Svecica	261	48			20.994	20.998	3	31	C
8770	Totanus	118	-67	294	-69	14.867			41	C
9299	Vinceteri	228	-63			87.95			22	E
10406	1997 WZ29	14	-86	184	-86	6.7520			22	E
10763	Hlawka	128	30			6.6833			21	E
10790	1991 XS	171	52	357	55	8.4894			33	C
! 11429	Demodokus	31	-77			50.23	50.16	2	25	E
! 11682	Shiwaku	25	68	206	74	4.01885			21	CE
12003	Hideosugai	32	-90			9.0157			27	E
12291	Gohnaumann	252	52			3.22070			22	C
13446	Almarkim	48	54	230	53	5.5116			25	E
13809	1998 XJ40	66	-27	225	-30	3.81363	40.256	2	22	E
14268	2000 AK156	119	-11			7.5121	7.51	3-	26	E
! 14362	1988 MH	188	6			3.64387	3.639	3	21	C
14376	1989 ST10	139	58	340	68	5.8481	5.614	3	28	E
! 14410	1991 RR1	342	-76			12.4272			32	E
15105	2000 BJ4	108	71			6.2570	6.257	2	29	CE
15496	1999 DQ3	23	89			81.21			27	E
15955	Johannesgmunden	327	-85			9.4985			22	E
16029	1999 DQ6	94	85			5.9537	5.95	3-	25	E
! 16771	1996 UQ3	49	63	253	41	4.95609			28	CE
17567	Hoshinoyakata	325	-87			19.891	19.882	2	22	E
18156	Kamisaibara	23	-88	221	-55	11.9166			24	C
18666	1998 FT53	316	49			5.5970			36	CE
20721	1999 XA105	74	-33	259	11	5.3478			34	C
! 21904	1999 VV12	225	73			5.4324			22	E
22972	1999 VR12	90	57			22.659			27	CE
! 24324	2000 AT51	132	53			5.8951			26	E
25846	2000 EF93	123	27	300	55	16.9713			29	E
32497	2000 XF18	214	15			24.578			22	E
40165	1998 QP102	331	86			7.4192	7.419	2	28	E
47678	2000 CT75	159	54			9.4505	9.453	2	23	E
! 51857	2001 OA105	78	59	257	29	4.31349	4.313	2	23	CE